ADVANCED MATERIALS
www.advmat.de

Low-Threshold Electrically Pumped Random Lasers

By *Hai Zhu, Chong-Xin Shan,* Ji-Ying Zhang, Zhen-Zhong Zhang, Bing-Hui Li, Dong-Xu Zhao, Bin Yao, De-Zhen Shen, Xi-Wu Fan, Zi-Kang Tang, Xianghui Hou,* and *Kwang-Leong Choy*

Random lasing is a phenomenon that has been discovered in some disordered media and extensive attention has been paid to this field in recent years. The topic has recently been addressed by Wiersma in a comprehensive review.[1] The attention on random lasers stems from both their fundamental scientific importance and their promising practical applications.[2–4] For example, random lasers usually exhibit a very broad angular distribution, thus are, in principle, ideal for display applications. Another unique advantage of random lasers compare with conventional lasers lies in thier low-cost and simple processing technology. They can be realized in coatings on surface of arbitrary shapes, thus find applications in display and lighting.[5,6] To date, most reported random lasers are obtained by optically pumping,[7–10] while only three research groups have realized electrically pumped random lasers, to the best of our knowledge, although those are highly desired.[11–14] Yu and co-workers have demonstrated electrically pumped random lasing from ZnO–SiO_2 nanocomposite.[11,12] The lasing, in their case, was realized in a complicated radial spreading structure. In a certain area of this structure, closed-loop cavities were formed and random lasing was realized there. One can see that the complication of this method impairs the unique advantages of random lasers. Chu et al. have recently demonstrated electrically pumped random lasing in a ZnO p–n junction.[13] It is widely accepted that p-type doping of ZnO is still a major challenge and the elaborate doping needed for such p–n junctions will also fade the unique advantages of random lasers. Moreover, since random lasing is usually realized in polycrystalline films or disordered media, the relatively poor structural quality makes intentional doping of the media almost impossible, which drastically hinders the realization of electrically pumped random lasing in p–n junctions. Actually, realizing electrically pumped random lasers in a facile route, which is crucial for display and lighting, has been one of the largest challenges for the future development of this kind of lasers. Ma *et al.* have realized an electrically pumped random laser in a simple Au/SiO_x/ZnO metal–oxide–semiconductor (MOS) structure.[14] However, the threshold in their case is very high (68 mA) and this high threshold will cause serious heating problems, which is adverse to the future applications of random lasers.

In this Communication, electrically pumped random lasers have been demonstrated in ZnO nanocrystallite films. The lasers were realized in a very simple way by coating several layers onto glass, and the threshold of the laser can be decreased to 6.5 mA by optimizing the hole-generation and injection configuration. The much-smaller threshold obtained and the simple structure employed in this Communication may present a significant step towards the practical applications of random lasers.

A typical scanning electron microscopy (SEM) topography of the ZnO films, used as the random lasing media here, is shown in Figure 1a. As can be seen, the films consist of nanocrystallites with sizes in the range of 30–50 nm. It has been reported that the optical gain of nanocrystalline ZnO is over one order of magnitude larger than that of bulk ZnO,[15,16] which is of great advantage in realizing lasers. Figure 1b illustrates the room-temperature photoluminescence (PL) spectrum of the ZnO films. As shown in the figure, the spectrum shows a dominant sharp near-band-edge (NBE) emission at around 380 nm, and the deep-level emission is almost undetectable. The X-ray diffraction (XRD) pattern of the ZnO films is shown in the inset of Figure 1b. Only one peak appears in the pattern, at 34.48°, which can be indexed to the diffraction from (0002) facet of wurtzite ZnO. The XRD data reveal that the ZnO films are hexagonal-wurtzite structured with *c*-axis-preferred orientation.

To realize electrically pumped random lasing, a MgO and Au layer were deposited onto the ZnO film in sequence to form an MOS structure. The schematic illustration of the structure is shown in Figure 2a. The thickness of the Au, MgO, and ZnO layer is 25, 50, and 150 nm, respectively. The Au contact was patterned into a circular pad with a diameter of 6 mm, using a shadow mask. Figure 2b shows the characteristic electroluminescence (EL) spectrum of the Au/MgO/ZnO structure under a continuous-current injection of 30 mA; the current–voltage (*I–V*) curve of the structure is illustrated in the inset. The spectrum is collected from the top face of the structure at room temperature. As shown in the figure, only one emission, centered at around 387 nm, can be

[*] Prof. C. X. Shan, H. Zhu, Prof. J. Y. Zhang, Dr. Z. Z. Zhang, B. H. Li, Prof. D. X. Zhao, Prof. B. Yao, Prof. D. Z. Shen, Prof. X. W. Fan
Key Laboratory of Excited State Processes
Changchun Institute of Optics, Fine Mechanics, and Physics
Chinese Academy of Sciences
Changchun 130033 (P. R. China)
E-mail: phycxshan@yahoo.com.cn
H. Zhu
Graduate School of the Chinese Academy of Sciences
Beijing 100049 (P. R. China)
Prof. Z. K. Tang
Department of Physics
Hong Kong University of Science & Technology
Clear Water Bay, Kowloon, Hong Kong (P. R. China)
Dr. X. H. Hou, Prof. K. L. Choy
School of Mechanical, Materials, and Manufacturing Engineering
The University of Nottingham
University Park, Nottingham, NG7 2RD (UK)

DOI: 10.1002/adma.200903623

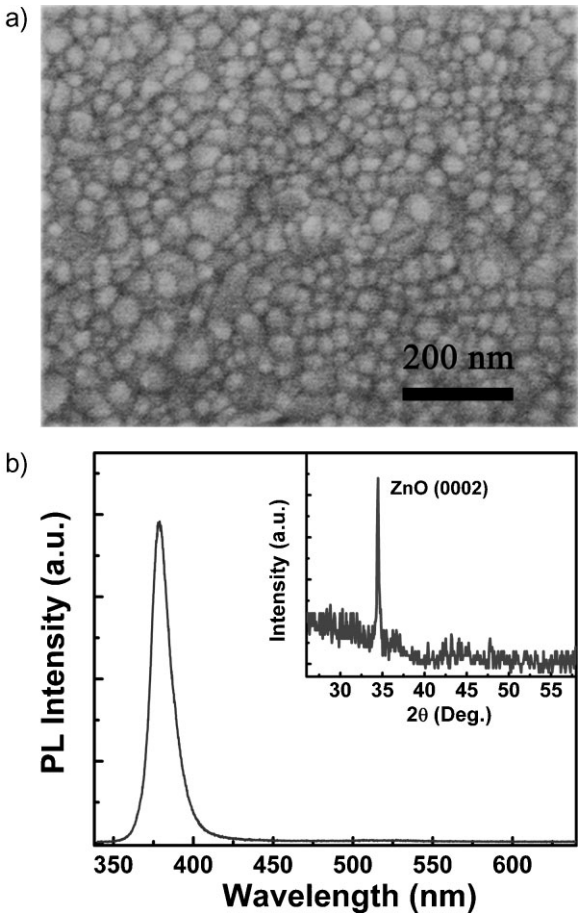

Figure 1. a) SEM topography of the ZnO nanocrystallite films grown on glass substrates. b) Room-temperature PL spectrum of the ZnO films. The inset shows the XRD pattern of the films.

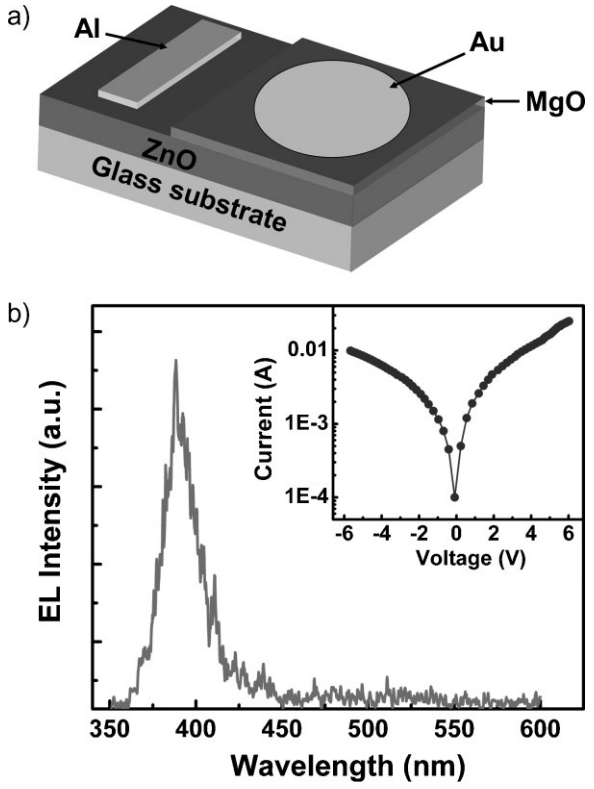

Figure 2. Schematic illustration (a) and EL spectrum (b) of the Au/MgO/ZnO structure under an injection current of 30 mA, the inset of Fig. 2b shows the *I–V* curve of the structure.

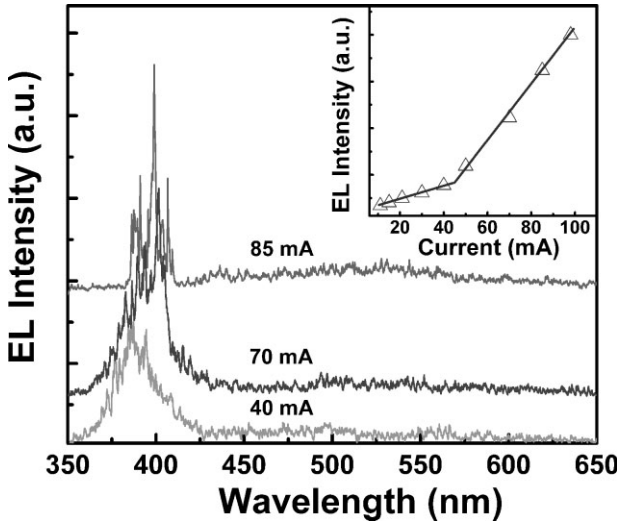

Figure 3. EL spectra of the Au/MgO/ZnO structure under different injection current. The inset shows the dependence of the integrated emission intensity of the structure on injection current.

observed in the spectrum, which corresponds to the NBE emission of ZnO, while the deep-level emission that is frequently observed in the EL of ZnO is invisible.

The room-temperature lasing characteristics of the Au/MgO/ZnO structure under the injection of continuous current are shown in Figure 3. When the injection current is 40 mA, a broad EL emission with its full width at half maximum (FWHM) of about 20 nm can be observed, while, as the current is increased to 70 mA, some sharp peaks superposed on the broad emission appear; the FWHM of these sharp peaks can be less than 0.8 nm. By further increasing the injection current to 85 mA, more such sharp peaks appear. The appearance of sharp peaks with very narrow linewidth upon increasing the injection current suggests that lasing action has been obtained. The dependence of the integrated emission intensity on the injection current is shown in the inset of Figure 3, from which a threshold current of about 43 mA can be derived.

To explore the origin of the EL, the band diagram of the Au/MgO/ZnO structure under forward bias is illustrated in Figure 4a. The conduction-band offset (ΔE_C) between ZnO and MgO is 3.55 eV,[17] which forms a barrier that prevents electrons in the ZnO layer from drifting to the Au electrode. As a result, electrons will accumulate at the MgO/ZnO interface driven by the forward bias. On the other hand, the electric field in the MgO layer is in the order of 10^6 V cm^{-1} at the threshold current by considering that most of the voltage will be applied onto the MgO layer due to its dielectric nature. Under such a high electric field,

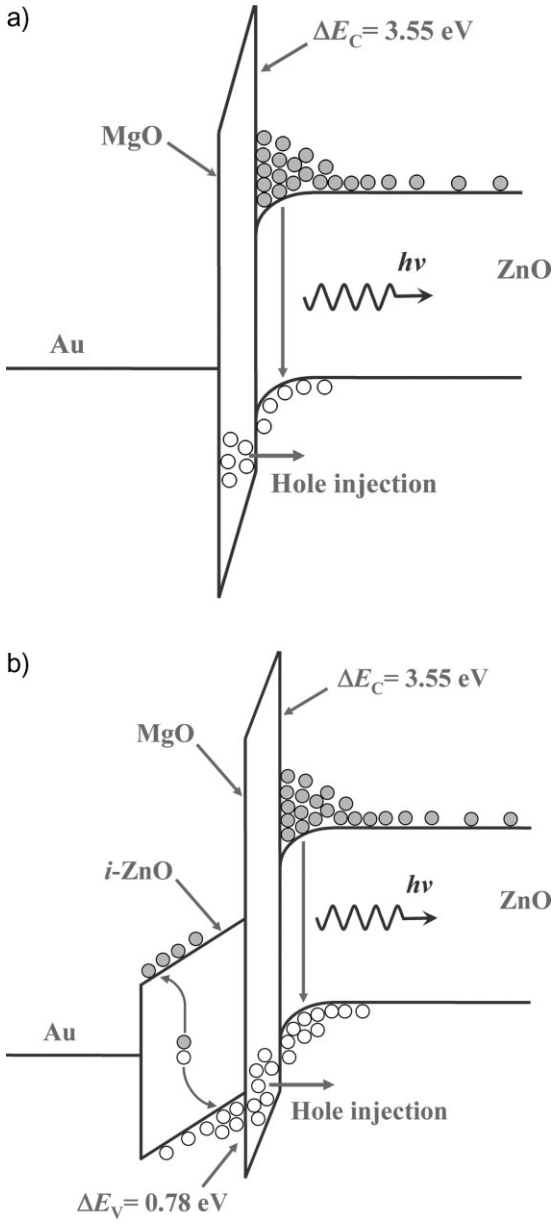

Figure 4. Schematic diagram showing the band alignment of the Au/MgO/ZnO structure (a) and the Au/i-ZnO/MgO/ZnO structure (b) under forward bias.

the carriers in the MgO layer, although they are few, will gain much energy and, under the drift of the electric field, they will impact with the lattice of the MgO layer, thus the electrons in the valence band will be excited. In this way, electrons and holes are generated by the impact-ionization process.[18] Under the forward bias, the generated holes can be injected into the ZnO layer and recombine radiatively with the electrons accumulated at the MgO/ZnO interface. As a result, emission from the structure can be observed. When the applied bias is increased to a certain value, where the optical gain is larger than the loss, lasing action is resulted.

As stated above, the injected holes are generated in the MgO layer via an impact ionization process under high electric field. It is demonstrated that the threshold ionization energy of a material is proportional to its bandgap.[19] The relatively large bandgap of MgO (7.7 eV) is a disadvantage for increasing the generation efficiency of holes in our case. It is thus rational to speculate that by replacing MgO with an insulator ZnO (i-ZnO), which has a smaller bandgap (3.37 eV), holes can be generated at a lower electric field, thus lasing with a lower threshold can be expected. Experimentally, an i-ZnO layer was introduced underneath the Au contact, and a Au/i-ZnO/MgO/ZnO metal–insulator–oxide–semiconductor structure is designed and prepared, the band alignment of which is shown in Figure 4b. In this structure, electron–hole pairs will be generated mainly in the i-ZnO layer at a relatively low electric field because of the much-smaller bandgap of ZnO compared to MgO, and the MgO layer acts merely as an electron-blocking layer that confines electrons in the ZnO layer. Considering the small valence-band offset (ΔE_V) between ZnO and MgO (0.78 eV),[20] the effective width of the MgO layer in the vicinity of valence-band offset will be greatly reduced due to the band bending of MgO caused by the bias applied. Thus, the generated holes in the i-ZnO layer can tunnel through the MgO barrier and enter into the ZnO layer driven by the bias. A similar situation can be found in our previous publication.[20] Since the threshold ionization energy has been lowered because of the smaller bandgap of ZnO, it is expected that the threshold of the laser will be greatly reduced in the Au/i-ZnO/MgO/ZnO structure compared with that in the Au/MgO/ZnO structure and an experimental confirmation on this speculation is discussed below.

The room-temperature EL spectra of the Au/i-ZnO/MgO/ZnO structure are shown in Figure 5. When the injection current is 5.0 mA, a broad EL emission with two broad emissions centered at about 400 and 530 nm can be observed. The emission at around 530 nm arises from the deep-level emission of the i-ZnO layer, while the one at around 400 nm corresponds to the NBE emission of the ZnO underneath the MgO layer. The red-shift of the NBE emission in this structure compared with that in the Au/MgO/ZnO structure is a result of the absorption of the high-energy side by the i-ZnO layer. Some sharp lines appear when the injection current is increased to 6.0 mA and they become more dominant when the injection current is further increased to 9.0 mA. The FWHM of these sharp peaks is less than 0.8 nm. The integrated intensity of the emission at around 400 nm versus the injection current is shown in the inset of Figure 5, from which a threshold current of about 6.5 mA can be derived. Note that the threshold is over one order of magnitude smaller than the only value reported in a similar Au/SiO_x/ZnO MOS structure (68 mA)[13] and is significantly smaller than the corresponding value obtained in the Au/MgO/ZnO structure (43 mA) mentioned above, which confirms that the i-ZnO layer indeed increases the generation efficiency of holes, thus lower-threshold lasing has been obtained, as expected. It is noted that the smaller threshold also helps to reduce the heating effect that is one of the largest troublesome issues in semiconductor lasers, thus is of great significance in the future applications of lasers.[21]

As for the lasing modes, considering that no elaborate resonant cavity is established in our experiment and that the thickness of

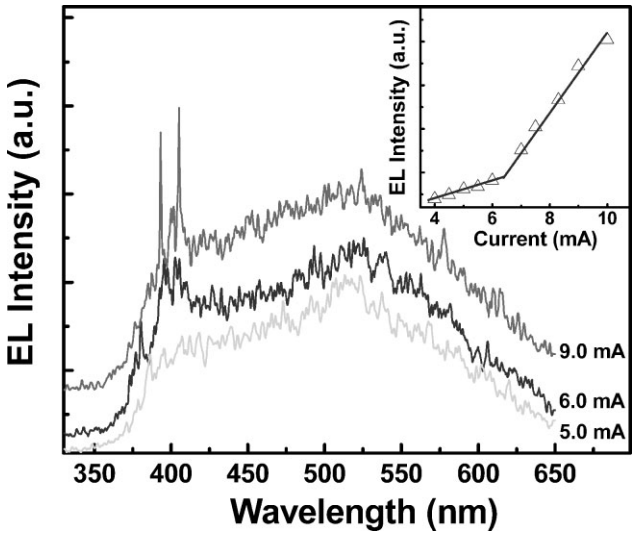

Figure 5. EL spectrum of the Au/i-ZnO/MgO/ZnO structure under different injection currents. The inset shows the integrated intensity of the emission at around 400 nm from this structure as a function of injection current.

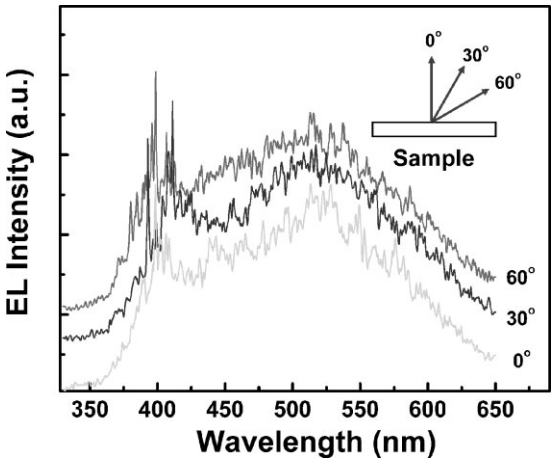

Figure 6. Lasing spectra of the Au/i-ZnO/MgO/ZnO structure observed at an angle of 0°, 30° and 60° in the plane normal to the film. The inset shows the schematic recording configuration.

the nanocrystallite films is about 150 nm smaller than the half-wavelength of the emitted light, the possibility that the lasing oscillation arises from a Fabry–Perot cavity can be excluded; thus, it is speculated that the lasing action observed in our case comes from a random laser. To confirm this speculation, the lasing spectra of the Au/i-ZnO/MgO/ZnO at different observation angles above the threshold have been measured. Figure 6 shows the lasing spectra observed at angles of 0°, 30°, and 60° in the plane normal to the film, and a schematic recording configuration is shown in the inset. One can see that lasing action has been observed in all the three recording configurations, although the spectra vary at different observation angles. The above phenomenon is very similar to the optically pumped random laser reported in ZnO by Cao et al.,[22,23] which confirms that the lasing oscillations observed in our case comes from a random laser.

The mechanism for random lasing in ZnO has been elucidated in literature.[2,24] Because the refractive index (n) of ZnO ($n = 2.45$) is much larger than that of air ($n = 1.0$), the light generated in the ZnO nanocrystallites undergoes a strong scattering process in the presence of grain boundaries.[8] In some cases, the emitted light can return to a scattering path from which it was scattered before; consequently, close-loop resonant cavities are formed. The optical gain can reach 571 cm^{-1}, while the loss can be as low as 68 cm^{-1} in ZnO crystallites.[25] The optical gain of the emitted light can exceed the loss in the close-loops at higher bias voltage in our case, and as a result lasing action occurs. Since the spatially distribution of the close-loop is random, lasing modes can be observed in many recording configurations. However, because the length of the close-loops can vary significantly, the lasing modes observed at different angles are significantly different. This is the reason why lasing oscillation has been observed but the mode varies greatly at different observation angles in our experiment shown in Figure 6.

In conclusion, electrically pumped random lasing has been realized in ZnO nanocrystallite films grown on glass substrates in a simple way. With the complement of an insulator-ZnO layer, the threshold current of the random laser can be decreased to 6.5 mA. Considering that the realization of electrically pumped lasing has been one of the largest challenges for future applications of random lasers, the results reported in this Communication, which provide a simple route to electrically pumped random lasers with an acceptably low threshold, may present a significant step towards future applications of this kind of lasers.

Experimental

The ZnO films were grown on a glass substrate in an atomic-layer-deposition technique. The detailed growth conditions can be found elsewhere [26]. Briefly, the precursors used were diethylzinc (DEZn) and water, and high-purity nitrogen was used as a carrier to lead the precursors into the growth chamber. The substrate temperature was fixed at 250 °C during the growth process. DEZn and water were pulsed into the growth chamber in sequence, and the pulse duration for DEZn and water was 15 and 10 microseconds, respectively. The precursors adsorbed on the surface of the substrate reacted and formed a ZnO monolayer. The excess precursors were exhausted for 3 s after each precursor pulse. The above growth cycle was repeated 1200 times and ZnO films with a thickness of about 150 nm were obtained. Then, a 50-nm MgO layer was deposited onto the ZnO films in a radio-frequency magnetron sputtering technique. Finally, a gold anode contact and an aluminum cathode contact were deposited onto the MgO and ZnO layer, respectively, by vacuum evaporation. The i-ZnO layer in the Au/i-ZnO/MgO/ZnO structure was prepared in a magnetron sputtering technique. The electron concentration and mobility of this layer are 2×10^{14} cm^{-3} and 4.0 cm^2 V^{-1} S^{-1}, respectively. The morphology of the ZnO films was characterized in a Hitachi S4800 field-emission SEM instrument. A Rigaku D/max-RA XRD with Cu Kα radiation was used to evaluate the crystalline properties of the ZnO films. PL spectra of the ZnO films were recorded in a JY-630 micro-Raman spectrometer using the 325-nm line of a He–Cd laser as the excitation source. EL measurements were carried out in a Hitachi F4500 spectrometer with a continuous-current power source. Note that all the measurements were performed at room temperature.

Acknowledgements

This work is supported by the "973" program (2006CB604906), the Knowledge Innovative Program of the Chinese Academy of Sciences (KJCX3.SYW.W01), the NNSFC (10774132, 50532050), the Science and Technology Developing Project of Jilin Province (20090124), and the Instrument Developing Project of the Chinese Academy of Sciences (YZ200903).

Received: October 22, 2009
Published online: February 12, 2010

[1] D. S. Wiersma, *Nat. Phys.* **2008**, *4*, 359.
[2] D. S. Wiersma, P. Bartolini, A. Lagendijk, R. Righini, *Nature* **1997**, *390*, 671.
[3] H. E. Türeci, L. Ge, S. Rotter, A. D. Stone, *Science* **2008**, *320*, 643.
[4] H. Cao, *Waves Random Media* **2003**, *13*, R1.
[5] D. S. Wiersma, *Nature* **2000**, *406*, 132.
[6] D. S. Wiersma, S. Cavalieri, *Nature* **2001**, *414*, 708.
[7] H. Cao, Y. G. Zhao, S. T. Ho, E. W. Seelig, Q. H. Wang, R. P. H. Chang, *Phys. Rev. Lett.* **1999**, *82*, 2278.
[8] J. Fallert, R. J. B. Dietz, J. Sartor, D. Schneider, C. Klingshirn, H. Kalt, *Nat. Photon.* **2009**, *3*, 279.
[9] S. Mujumdar, V. Tuerck, R. Torre, D. S. Wiersma, *Phys. Rev. A* **2007**, *76*, 033807.
[10] S. F. Yu, C. Yuen, S. P. Lau, H. W. Lee, *Appl. Phys. Lett.* **2004**, *84*, 3244.
[11] E. S. P. Leong, S. F. Yu, *Adv. Mater.* **2006**, *18*, 1685.
[12] E. S. P. Leong, S. F. Yu, S. P. Lau, *Appl. Phys. Lett.* **2006**, *89*, 221109.
[13] S. Chu, M. Olmedo, Z. Yang, J. Y. Kong, J. L. Liu, *Appl. Phys. Lett.* **2008**, *93*, 181106.
[14] X. Y. Ma, P. L. Chen, D. S. Li, Y. Y. Zhang, D. R. Yang, *Appl. Phys. Lett.* **2007**, *91*, 251109.
[15] Z. K. Tang, G. K. L. Wong, P. Yu, M. Kawasaki, A. Ohtomo, H. Koinuma, Y. Segawa, *Appl. Phys. Lett.* **1998**, *72*, 3270.
[16] P. Zu, Z. K. Tang, G. K. L. Wong, M. Kawasaki, A. Ohtomo, H. Koinuma, Y. Segawa, *Solid State Commun.* **1997**, *103*, 459.
[17] S. J. Jiao, Y. M. Lu, D. Z. Shen, Z. Z. Zhang, B. H. Li, J. Y. Zhang, B. Yao, Y. C. Liu, X. W. Fan, *Phys. Stat. Sol. C* **2006**, *4*, 972.
[18] S. M. Sze, *Physics of Semiconductor Devices*, 2nd ed. Wiley, New York **1981**.
[19] J. L. Hudgins, G. S. Simin, E. Santi, M. A. Khan, *IEEE Trans. Power Electron.* **2003**, *18*, 907.
[20] H. Zhu, C. X. Shan, B. Yao, B. H. Li, J. Y. Zhang, Z. Z. Zhang, D. X. Zhao, D. Z. Shen, X. W. Fan, Y. M. Lu, Z. K. Tang, *Adv. Mater.* **2009**, *21*, 1613.
[21] L. A. Coldren, S. W. Corzine, *Diode Lasers and Photonic Integrated Circuits*, Wiley, New York **1995**.
[22] H. Cao, Y. G. Zhao, H. C. Ong, S. T. Ho, J. Y. Dai, J. Y. Wu, R. P. H. Chang, *Appl. Phys. Lett.* **1998**, *73*, 3656.
[23] H. Cao, Y. G. Zhao, H. C. Ong, R. P. H. Chang, *Phys. Rev. B* **1999**, *59*, 15107.
[24] H. Cao, J. Y. Xu, S. H. Chang, S. T. Ho, *Phys. Rev. E* **2000**, *61*, 1985.
[25] X. Q. Zhang, Z. K. Tang, M. Kawasaki, A. Ohtomo, H. Koinuma, *J. Crystal Growth* **2003**, *259*, 286.
[26] C. X. Shan, J. Y. Zhang, B. Yao, D. Z. Shen, X. W. Fan, K. L. Choy, *J. Vac. Sci. Technol. B* **2009**, *27*, 1765.